Paper AAS 04-277

DYNAMICS AND CONTROL OF A HERD OF SONDES GUIDED BY A BLIMP ON TITAN

Marco B. Quadrelli, Johnny Chang, and Scott Kowalchuck

14th AAS/AIAA Space Flight Mechanics Conference

Maui, Hawaii, February 8-12, 2004

AAS Publications Office, P.O. Box 28130, San Diego, CA 92198

Paper 04-277

DYNAMICS AND CONTROL OF A HERD OF SONDES GUIDED BY A BLIMP ON TITAN[1]

Marco B. Quadrelli[2], Johnny Chang, and Scott Kowalchuck

This paper describes the model and the algorithm developed for an aerobot blimp guiding and controlling a herd of sondes on the surface of Titan. The paper summarizes the derivation of the equations of motion used in simulations, and the features of the simulation model. A potential field controller is used for autonomous guidance and navigation around terrain features on the surface, and hazard avoidance. The results of simulation studies demonstrate that the method used for control is feasible even if significant uncertainty exists in the dynamics and environmental models, and that the control method provides the autonomy needed to enable surface science data collection.

Introduction

We address the problem of autonomous operation of a herd of cooperating vehicles deployed in unknown planetary environments (Titan, Mars, Venus) for in-situ sampling and data collection. This concept is a viable candidate for all future planetary exploration missions targeting scientific returns in areas such as surface geology and tropospheric or stratospheric sampling. In particular, we address a herd or flock of mobile sensors deployed in a totally unknown environment that must be reconfigured or repositioned to a more favorable location (providing more scientific throughput, better coverage, etc). In our approach, a herd leader (blimp) is selected, and the rest of the herd of mobile vehicles autonomously tracks the commands of the leader. We propose a potential field approach for autonomous command and control, and a centralized estimation scheme for intra-herd range determination. Inertial knowledge is acquired via land radio beacons and via Direct to Earth communication. With our algorithm, the blimp and surface sondes redistribute appropriately despite the uncertain environment. Numerical results show the performance and robustness of the algorithms in the distributed simulation testbed developed for this application, and show the promise of the approach for future missions.

---

[2] Corresponding author, Mail Stop 198-326, Jet Propulsion Laboratory, California Institute of Technology, 4800 Oak Grove Drive, Pasadena, CA 91109-8099, E-mail: marco@grover.jpl.nasa.gov

This paper first describes the model and the algorithm developed for the Titan aerobot blimp guiding and controlling a herd of sondes on the planet's surface, the derivation of the equations of motion used in the simulation, and the details of the simulation model are summarized. These dynamics and control models of the blimp and sondes are quite general. A potential field controller is used for autonomous tracking of terrain features on the surface, and hazard avoidance. Simulation studies demonstrate that this method of control is feasible even if significant uncertainty exists in the dynamics and environmental models.

The objectives of the model development are: 1) to enable parametric studies; and 2) to conceive and test possible control options for herd trajectory & attitude control and for sample capture scenario. This was accomplished by a progressive build-up of models of increasing complexity, namely: 1) first order models, 2) quick order-of-magnitude determinations, 3) point mass, enabling ascent/descent and trajectory analysis, 4) few parameters, simple to handle, full six-degrees-of-freedom, enabling simulation studies, and 5) lots of parameters, difficult to handle, multibody models.

While Titan has a surface pressure of 1.5atmos and an atmosphere mostly N2 like Earth, its low gravity and inverted atmospheric temperature (i.e., 70-90K from the surface up to 50km, but >115K above 75km) mean that the atmosphere is saturated—it rains organics. The primary science goals are as follows: 1) sample the Titan atmosphere near the surface; 2) sample the organic rich lakes both at the surface and subsurface, sampling the bottom material; and 3) sample the solid organic rich ice at the rims of cratered lakes.
Given the science requirement to sample atmosphere, liquids, and solids over a wide region, the best design for a probe revolved around an amphibious sonde which could be free swimming or tethered—the vehicle would be deployed off the aerial platform. There are two primary surface instrument delivery options being considered:
1. The aerial platform does an aerial survey of a large area first before selecting a prime science target (i.e., a cratered organic lake with rich rim deposits of organic precipitates and mineralogy)---three sondes are separately deployed (one tethered for analyzing the atmospheric column, one free swimming for subsurface liquid column analysis, and one crawler for crater rim solids analysis);
2. The aerial platform carries one tethered deployable sonde which samples the atmospheric column, samples the liquid lakes, and samples the crater rim material as the aerial platform moves from site to site.

The mission under consideration (described in detail elsewhere [1]) takes place in the 2020 time frame, after Cassini-Huygens has generated a sufficient wealth of knowledge about Titan that an in-situ exploration of Saturn's moon becomes imperative for planetary science. After a direct entry, a total payload mass of 300 Kg is slowed down by a parachute until the moment of blimp inflation. Once the blimp is at stable float altitude (between 1 and 6 km altitude), and a site of scientific interest is identified, the blimp descends to the surface, drops the three-sonde package (herd), and from then on guides the herd to different locations after processing images of the terrain. The uncertainty of the terrain morphology on Titan is large. Hence the sondes need mobility on the surface

as well as under the surface (as an amphibious vehicle). Figure 1 depicts an artist's rendition of this scenario.

First, the blimp model is described. Second the sonde model is described. Third, the integrated simulation environment is described, with emphasis on the distributed sensing and actuation architecture used to command and control the herd of sondes. Finally, several simulation results are analyzed. The result of simulation studies demonstrate that the method used for commanding the herd (based on a potential field architecture), and for the distributed sensing of the herd based on transmitting and receiving radio-frequency signals amongst the vehicles is feasible even if significant uncertainty exists in the dynamics and environmental models. These results are very encouraging, and open the way to efficient autonomous control of many data gathering vehicles in unknown planetary environments.

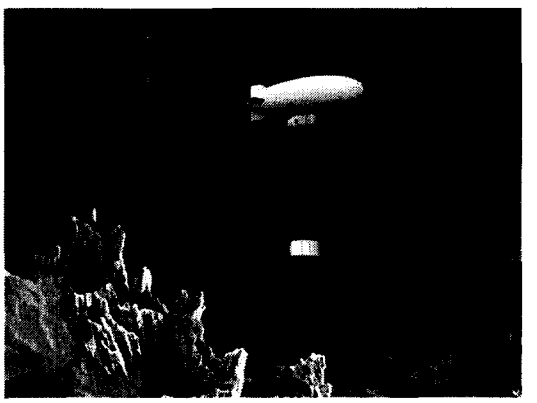

Figure 1. The Titan blimp dropping one of the sondes on an icy lake.

Cooperation Architecture

The objective of the concept being described in this paper is to demonstrate active cooperative control of herds of mobile sondes in Titan's environment to increase autonomy and direct herd towards a common goal. Controlling cooperative sensor herds is a critical technology for autonomous planetary sampling. Our approach is to develop algorithms/techniques for cooperative, distributed sensing and control of multiple sondes in Titan's environment, and to demonstrate our concept in simulation.

While multiple robots offer excellent opportunities for distributed scientific data collection. Efficient collection of distributed science information requires deploying many sensor packages/units in different locations. These locations may be characterized by hazards such as active vents/ice flows, floating ice masses, unpredictable local environmental flows or terrain features, and different illumination conditions.

Multiple Robots are advantageous since they: 1) can manage homogeneous vs. heterogeneous herd, 2) have the capability to model other agents in herd, 3) can interact via sensing (kin recognition), 4) can interact via communication (network topology & comm. protocols), and 5) can interact via the environment (cooperation without communication).

We define cooperation as follows: given a specific task, a herd displays autonomous collaborative behavior if, due to some underlying mechanism of cooperation, there is a net increase in the total utility of the system. Cooperation involves: addressing homogeneity/heterogeneity of vehicles, task decomposition, task allocation among members, fault-tolerance and hazard avoidance, distributed sensing and communication, reasoning, i.e. inference of what other vehicles think, non-intersecting path-planning, learning aspect and self-organized behavior, and possible conflict management. The herd's objective is to accomplish a specific task, namely: to collect as much scientific data of interest, from as many locations as possible, and return sample to origin. In the case of Titan's exploration, the main goals are to explore the atmosphere in order to understand the climate and atmosphere composition of Titan, to explore the surface to understand the geophysics and mineralogy of Titan, and to collect and analyze a sample in-situ, and possibly return it to Earth.

Cooperation may be the result of genetically determined individual behavior (or eusocial), or it may be the result of social interactions between selfish agents. In any case, representative cooperation architectures are: 1) CBOTS (Cellular roBOTics System), which is bioinspired, decentralized, 2) SWARM, which is distributed with large number of agents, and 3) ALLIANCE, which is small to medium size heterogeneous teams. The learning process may be reinforcement-based, to adapt to changes in environment, with the goal of evolving flocking behavior, or to resolve resource conflict. However, formal metrics for cooperation and system performance, and for grades of cooperation, are still missing.

Lack of effective sensors can render the cooperation paradigm very difficult to implement. Collective robotics must deal with all of the HW/SW problems of single-robotics systems, complicated by the multiplicity factor. Use of GPS-like sensors can compensate for limited vision of agents, but can place severe environmental constraints under which agents operate, due to interference paths.

Some *qualitative* metrics for performance of Autonomous Robots are related to 1) maintaining the desired formation dynamics (deviation from template: % distance, % bearing), 2) the degree of independence of decision making for each element (limit no. of queries to centralized leader requesting commands for action), 3) the survivability of each element in unknown environment (successfully negotiate obstacles, communicate through obscurations), and 4) the capability of assuming leader role when needed (move from centralized to decentralized architecture).

The herd cooperation challenges that we have identified are: formation relative sensing and control, synchronous herd reconfiguration and reorientation, power optimality, centralized or decentralized distributed control and estimation, reliable actuation/sensing mechanisms, tolerant to environmental uncertainty, distributed communication, crosslinks, downlinks, high speed distributed computing, data management & autonomy, collaborative behavior, autonomous fault detection/recovery, coordinated instruments and science planning/processing, asynchronous processing.

Blimp Kinematics and Dynamics

The objectives of the blimp and sondes model development are to enable parametric studies and to conceive and test possible control options for the blimp and sondes during the surface science scenario. Several bodies can be accommodated: blimp, multiple sondes.

The assumptions and features of the blimp model are as follows. The blimp is modeled by a rigid body. Blimp ascent/descent and trajectory studies can be carried out via thrust vectoring the blimp propellers, or via differential volume change of the ballonets inside the blimp. The blimp attitude dynamics are parameterized by Euler angles, measuring the attitude with respect to a Titan centered frame. Titan is modeled as a flat plane. The simulation model can apply lateral and vertical components of a wind gust profile to the blimp. Blimp aerodynamic and added mass coefficients are obtained from tests reported in literature. Thrusting devices (propellers) are modeled by a point force/torque (and may be articulated for thrust vectoring). A tether-line connecting the blimp to a sonde is represented by a visco-elastic tether link of variable length. Sensor models and estimators include a star tracker, accelerometers, and gyro. Actuator models are included as a first order lag. Tracking control laws include proportional, derivative, and feedforward control terms. Blimp modeling is very complex due to a center of mass located below the center of volume (gas enclosed within envelope), variable mass and inertia due to inflating/deflating ballonets, thrust-vectored propellers, changing center of pressure due to geometric asymmetry, and moving control surfaces. We make some simplifications, assuming a rigid envelope, fixed center of volume and center of mass, and no ballonets present.

The translation and rotation kinematics equations for a six degree of freedom model of the blimp can be written as:

$$\begin{pmatrix} \dot{R}_x \\ \dot{R}_y \\ \dot{R}_z \end{pmatrix} = A_z(-\psi)A_y(-\theta)A_x(-\phi)\begin{pmatrix} u \\ v \\ w \end{pmatrix} \tag{1}$$

$$\begin{pmatrix} \dot{\phi} \\ \dot{\theta} \\ \dot{\psi} \end{pmatrix} = \begin{bmatrix} 1 & \tan\theta\sin\phi & \tan\theta\cos\phi \\ 0 & \cos\phi & -\sin\phi \\ 0 & \dfrac{\sin\phi}{\cos\theta} & \dfrac{\cos\phi}{\cos\theta} \end{bmatrix} \begin{pmatrix} p \\ q \\ r \end{pmatrix} \tag{2}$$

$$\begin{aligned} u &= V\cos\beta\cos\alpha \\ v &= V\sin\beta \\ w &= V\cos\beta\sin\alpha \end{aligned} \tag{3}$$

$$\begin{aligned} &\tan\alpha = w/u \\ &\sin\beta = v/V \\ &V^2 = (u - W_x)^2 + (v - W_y)^2 + (w - W_z)^2 \end{aligned} \tag{4}$$

where A_X, A_Y, A_Z= rotation matrices about inertially fixed axes (X,Y,Z), R_X, R_Y, R_Z= components of distance of the blimp's center of volume from Titan's origin, ψ=attitude yaw angle of flight vehicle with respect to local tangent plane on the surface of Titan, θ = attitude pitch angle of flight vehicle with respect to local tangent plane, ϕ, = attitude roll angle of flight vehicle with respect to local tangent plane, u = velocity component along body-fixed x-axis, v = velocity component along body-fixed y-axis, w = velocity component along body-fixed z-axis, p, q, r denote the body frame components of the angular velocity of the blimp, α = angle of attack, β = angle of sideslip, and W_X, W_Y, W_Z = components of wind speed in body frame.

The translation and rotation equations of motion of the blimp may be written as:

$$\begin{aligned} &(m - X_{\dot{u}})\dot{u} = (m - Y_{\dot{v}})rv - (m - Z_{\dot{w}})qw + m\left[d_x(r^2 + q^2) - d_z pr\right] - (md_z - X_{\dot{q}})\dot{q} + \left[-mg(\frac{R_\oplus}{R_\oplus + h})^2 + B\right]\sin\theta + X + T_x \\ &(m - Y_{\dot{v}})\dot{v} = (m - Z_{\dot{w}})pw - (m - X_{\dot{u}})ru + m\left[-d_x pq - d_z pr\right] - (md_x - Y_{\dot{r}})\dot{r} - (-md_z - Y_{\dot{p}})\dot{p} + \left[mg(\frac{R_\oplus}{R_\oplus + h})^2 - B\right]\cos\theta\sin\phi + Y + T_y \\ &(m - Z_{\dot{w}})\dot{w} = (m - X_{\dot{u}})qu - (m - Y_{\dot{v}})pv + m\left[-d_x pr + d_z(p^2 + q^2)\right] + (-md_x - Z_{\dot{q}})\dot{q} + \left[mg(\frac{R_\oplus}{R_\oplus + h})^2 - B\right]\cos\theta\cos\phi + Z + T_z \end{aligned} \tag{5}$$

$$\begin{aligned} &(J_{xx} - L_{\dot{p}})\dot{p} = -(J_{zz} - J_{yy})qr + J_{xz}(\dot{r} + pq) + md_z(ur - wp) + (-md_z - L_{\dot{v}})\dot{v} + L + L_T + B_p + W_p \\ &(J_{yy} - M_{\dot{q}})\dot{q} = -(J_{xx} - J_{zz})pr + J_{xz}(r^2 - p^2) + md_x(vp - uq) - md_z(wq - vr) - (md_z - M_{\dot{u}})\dot{u} - (-md_x - M_{\dot{w}})\dot{w} + M + M_T + B_q + W_q \\ &(J_{zz} - L_{\dot{r}})\dot{r} = -(J_{yy} - J_{xx})pq + J_{xz}(\dot{p} - qr) - md_x(ur - wp) + (md_x - N_{\dot{v}})\dot{v} + N + N_T + B_r + W_r \end{aligned} \tag{6}$$

$$L = q_d SbC_l$$
$$M = q_d ScC_m \tag{7}$$
$$N = q_d SbC_n$$

where: m is the blimp's mass, S the blimp's reference area, b and c the long and short axes of an equivalent ellipsoid representing the blimp's envelope, Jxx, Jyy, Jxx, Jxz = total vehicle moments of inertia (may include ballonets of variable inertia), d_x, d_z = distances from center of mass to center of volume in body frame, q_d is the dynamic pressure, Bp, Bq, Br = components of torque due to buoyancy B in body frame, Wp, Wq, Wr = components of weight torques in body frame, CL, Cm, Cn, are blimp aerodynamic coefficients, L, M, N = aerodynamic force moments in body frame, Tx, Ty, Tz are body fixed components of the thrust vector, LT, MT, NT = components of thrust moment in body frame, $X_{\dot{u}}, Y_{\dot{v}}, Z_{\dot{w}}, L_{\dot{p}}, M_{\dot{q}}, N_{\dot{r}}$ = components of added mass forces and moments in body frame, and $R_{\oplus}$ is Titan's equatorial radius. The dynamics equations are inertially coupled by center of mass to center of volume offset, by asymmetry in x-z plane, and by added mass force and moment coefficients.

A software database has been created using aerodynamic parameters of the YEZ airship. These parameters are derived from wind tunnel data from 1990 initially obtained at Cranfield Institute of Technology, England. The lift, drag, and side forces and roll, pitch, and yaw moments are a function of angle-of-attack α, sideslip angle β, elevator angle η, aileron angle ζ, and rudder angle ε. These equations compute η, ζ, and ε from the 4 control surfaces of the blimp (Figure 2 and Table 1):

$$\eta = \frac{\delta_1 + \delta_2 + \delta_3 + \delta_4}{4}$$
$$\varsigma = \frac{\delta_1 - \delta_2 + \delta_3 - \delta_4}{4} \tag{8}$$
$$\varepsilon = \frac{\delta_1 - \delta_2 - \delta_3 + \delta_4}{4}$$

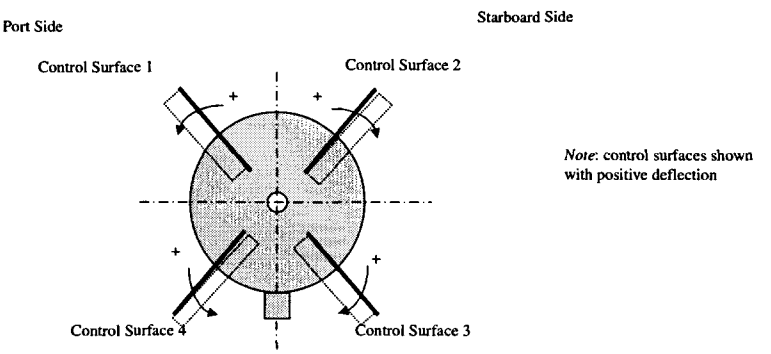

Figure 2. Blimp Control Surface Deflection Sign Convention as Viewed from the Stern.

Table 1: Maneuver Response with Control Surface Deflection

Maneuver	Condition	η	ς	ε
Pitch Up	$\delta_1+\delta_2+\delta_3+\delta_4>0$	+	+ or -	+ or -
Pitch Down	$\delta_1+\delta_2+\delta_3+\delta_4<0$	-	+ or -	+ or -
Yaw Left	$\delta_1-\delta_2+\delta_3-\delta_4>0$	+ or -	+	+ or -
Yaw Right	$\delta_1-\delta_2+\delta_3-\delta_4<0$	+ or -	-	+ or -
Roll Left	$\delta_1-\delta_2-\delta_3+\delta_4<0$	+ or -	+ or -	-
Roll Right	$\delta_1-\delta_2-\delta_3+\delta_4>0$	+ or -	+ or -	+

From the experimental data, we obtained surface fits of 3D aerodynamic data in analytical form as follows:

$$C_{total}(\alpha,\beta)=\begin{bmatrix}C(\alpha,\beta)_\eta & C(\alpha,\beta)_\varepsilon & C(\alpha,\beta)_\varsigma\end{bmatrix}\begin{bmatrix}a\eta^2+b\eta+c\\ a\varepsilon^2+b\varepsilon+c\\ a\varsigma^2+b\varsigma+c\end{bmatrix} \tag{9}$$

This step provides a direct analytical mapping between control forces and moments, and control surface deflections. This mapping is very useful for control surfaces design and for control system specification. The mappings are shown in Figure 3.

The blimp actuators are: two thrust vectored propellers (pitch axis can be varied) on the right and left sides of the blimp, one fixed push propeller on the back, four internal ballonets for buoyancy control, and rudder and elevators in the tail. The blimp sensor complement includes: a star tracker, an inertial measurement unit (IMU), an accelerometer, as well as temperature and pressure sensors. The thermal control of the blimp is very demanding, since the vehicle operates in a cryogenic environment (77K on the surface of Titan) and the blimp would be powered by a radioisotope power source (RPS).

We analytically parameterized the tail fin aerodynamics by changing the tail fin aspect ratio, and observing the response on the aerodynamic coefficients. We observed that: 1) the curves are approximately contained inside limits of fully equipped hull (FH) and bare hull (BH) curves, as it should be; 2) variations within these limits are presumably due to other protuberances besides tail fins (gondola, propeller ducts, others); 3) stability in pitch and yaw is immediately achieved, and is largely improved by adding fins, as expected; 4) there is no significant increase in drag at zero α, but decrease at high α instead, probably due to having chosen a reference drag coefficient $(C_{Df})_0$ =0.01 (an inflated profile would likely increase drag much more at near zero α); 5) normal and side force coefficients increase at large α, as expected; 6) rolling moment is unaffected by

parameterization, but in reality there should be a small change. Figure 4 depicts the parameterized aerodynamic coefficients, as a function of tail fin aspect ratio.

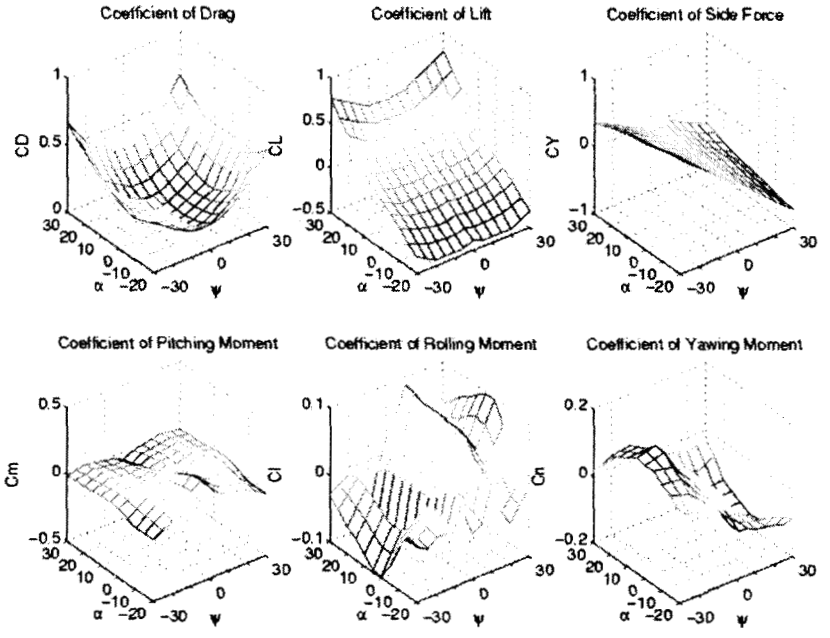

Figure 3. Blimp Aerodynamic coefficients (for elevator=[-16.25 deg], aileron=[1.25 deg], rudder=[-3.75 deg] deflection).

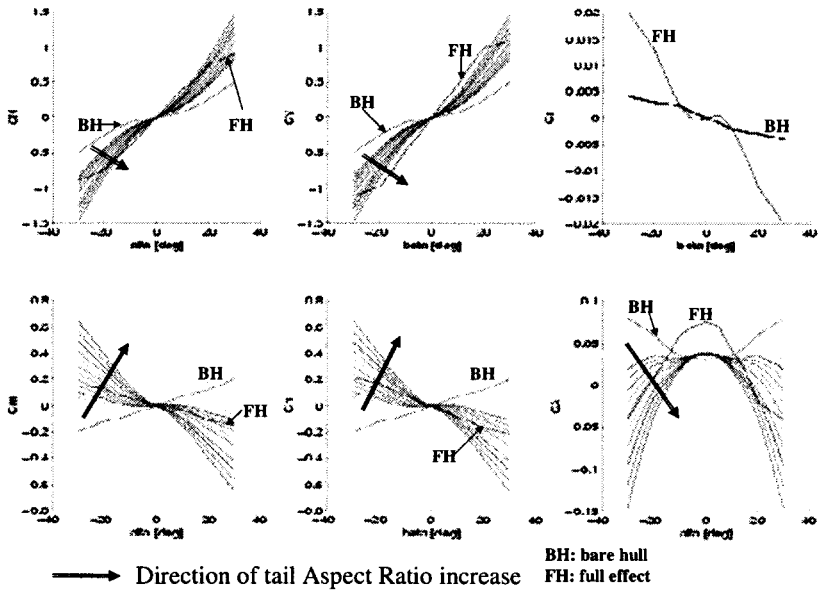

Figure 4. Parameterized Tail Fin Aerodynamics.

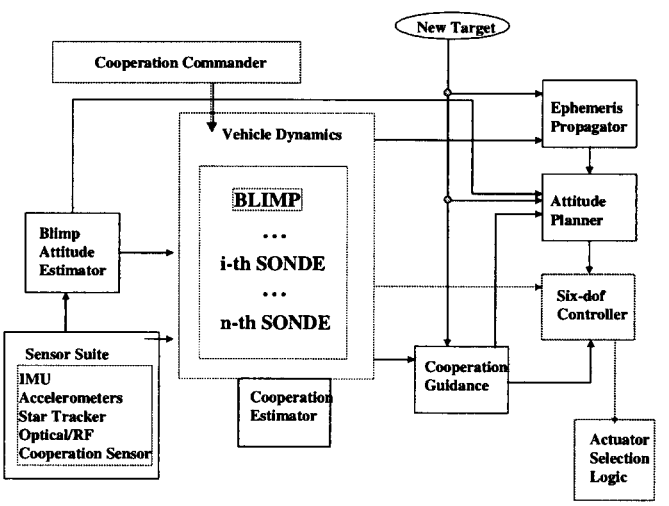

Figure 5. A functional diagram of the integrated simulation.

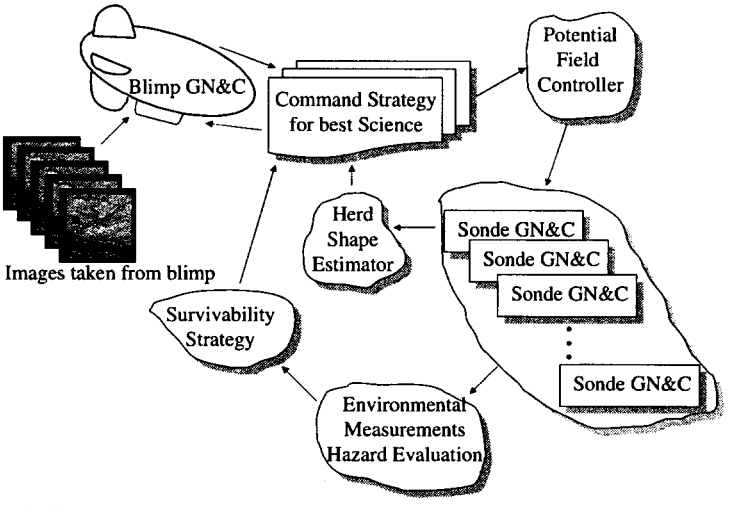

Figure 6. Conceptual Image-based Guidance & Control of Titan's herd.

Planar Sonde Kinematics and Dynamics

In this section, we discuss the sonde model used in our simulation. We simplify our sonde model as a non-holonomic mobile robot with two actuated wheels [3,4]. The steering is achieved with the difference in speed of the two wheels. Consider the planar model in figure 7.

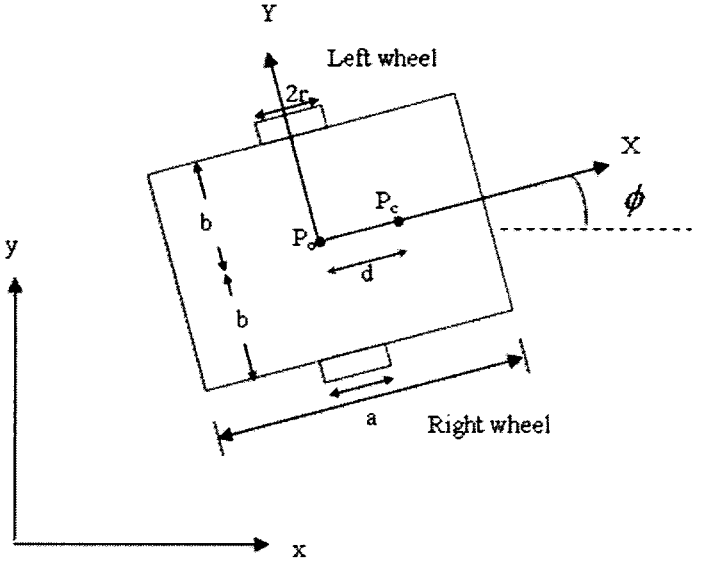

Figure 7. Planar sonde model.

The mobile robot in figure 7 can be described by the following five generalized coordinates: $q = [x, y, \phi, \theta_r, \theta_l]^T$, where (x, y) is the world coordinate of P_o, the center of the robot, ϕ is the rotational angle of the body x-axis (forward vector), and θ_r, θ_l are the wheel angles. P_c is the center of the mass of the robot, 2a is the length, and 2b is the width of the robot, r is the radius of the wheels, d is the distance of P_c from P_o. Assuming that the wheels do not slip, we conclude that the velocity of robot is constrained in the direction of the axis of symmetry. The constraints can be written as:

$$\begin{aligned} &\dot{y}\cos\phi - \dot{x}\sin\phi = 0 \\ &\dot{x}\cos\phi + \dot{y}\sin\phi + b\dot{\phi} = r\dot{\theta}_r \\ &\dot{x}\cos\phi + \dot{y}\sin\phi - b\dot{\phi} = r\dot{\theta}_l \end{aligned} \tag{10}$$

In matrix form: $A(q)\dot{q} = 0$, where

$$A(q) = \begin{bmatrix} \sin\phi & -\cos\phi & 0 & 0 & 0 \\ \cos\phi & \sin\phi & b & -r & 0 \\ \cos\phi & \sin\phi & -b & 0 & -r \end{bmatrix} \tag{11}$$

We can then express the equation of motion as follows:

$$\begin{aligned} &\dot{q} = S(q)v(t) \\ &M(q)\dot{v} + V(q,\dot{q})v = B(q)\tau \end{aligned} \tag{12}$$

where

$$S(q) = \begin{bmatrix} \frac{r}{2}\cos\phi & \frac{r}{2}\cos\phi \\ \frac{r}{2}\sin\phi & \frac{r}{2}\sin\phi \\ \frac{r}{2b} & -\frac{r}{2b} \\ 1 & 0 \\ 0 & 1 \end{bmatrix} \tag{13}$$

$$M = \begin{bmatrix} \frac{r^2}{4b^2}(mb^2 + I) + I_w & \frac{r^2}{4b^2}(mb^2 - I) \\ \frac{r^2}{4b^2}(mb^2 - I) & \frac{r^2}{4b^2}(mb^2 + I) + I_w \end{bmatrix} \tag{14}$$

$$V = \begin{bmatrix} 0 & \frac{r^2}{2b} m_c d\dot{\phi} \\ -\frac{r^2}{2b} m_c d\dot{\phi} & 0 \end{bmatrix} \tag{15}$$

$$B = \begin{bmatrix} 1 & 0 \\ 0 & 1 \end{bmatrix} \tag{16}$$

The torques acting on the right and left wheels are $\tau = [\tau_r, \tau_l]^T$, and $m = m_c + 2m_w$,

$$I = m_c d^2 + 2m_w b^2 + I_c + 2I_m \tag{17}$$

where m_c is the mass of the body, and m_w is the mass of a wheel.

$$M(q)\ddot{q} + V(q,\dot{q})\dot{q} + G(q) = B(q)\tau + A^T(q)\lambda \tag{18}$$

All vehicles, blimp and sondes, are assumed to have similar sensor suite and sensor performance. Each vehicle in our model is equipped with an accelerometer, a gyro, and an inertial attitude measurement unit (inclinometer, possibly a star tracker). Random noise is added to the acceleration computed from the dynamics. The following accelerometer model parameters are used in the simulation: 1) standard deviation of accelerometer measurement noise: 35μg; 2) Accelerometer saturation: 40g; 3) Variance of gyro measurement noise: (1-σ); 4) Standard deviation of gyro angle random walk: std = 0.07 deg/(hr)$^{1/2}$; 5) Standard deviation of gyro bias drift = 1.0 deg. /hr (100s correlation time). For the attitude sensor located on the blimp, the assumed variance of star tracker measurement noise (1- σ) is 3 arc-sec.

Figure 5 shows a functional diagram of the integrated simulation environment. Figure 6 shows the image-in-the-loop driven commander, which resides in the blimp, and a conceptual guidance and control scheme for guiding the herd. After Commands are given to the sondes by the blimp, the controller is activated. The Controller is split into the control of the separated sondes in the form of attitude and position control forces and torques, and into the potential field (cooperation) controller. The control inputs are filtered by the dynamics and noise models of the actuators. The noisy control inputs are then used in the Dynamics module, which propagates the state of the entire herd, and in addition provides updates of the inertial state and of the environmental perturbations acting on the system. The dynamic state is subsequently manipulated by the Sensor Models, which reproduce sensor measurements with noise (Star Tracker, Accelerometers, Gyros, and Laser and Radio Frequency-based metrology). With the measurements

available, the cooperation estimator can now provide estimates of the relative herd state, which is then delivered to the Commander to close the cycle. The Sensor models and Estimators, including the Cooperation Estimator, run in discrete time, whereas the Commander, Controller, and Dynamics modules run in continuous time, making this simulation a hybrid discrete-continuous simulation.

Cooperation Estimator

Figure 8 depicts the sonde-blimp intra-herd distributed communication topology, using radio-frequency signals. Figure 9 shows the essential elements of the cooperation estimator, which uses the network depicted in Figure 8 to process intra-herd variables for purposes of estimating the current relative state of the entire herd of vehicles. The distributed relative sensing element is based on Cooperation Sensor Ka-Band Transceivers/Patch Antennas, which provides range and bearing and full-duplex links between: blimp and sonde, and sonde to sonde. Additional links can be added for fault protection and collision avoidance.

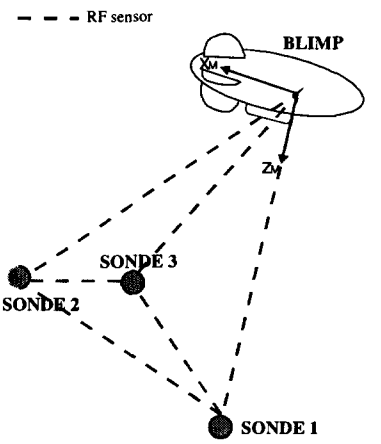

Figure 8. Sonde-Blimp Intra-herd Distributed Communication Plan..

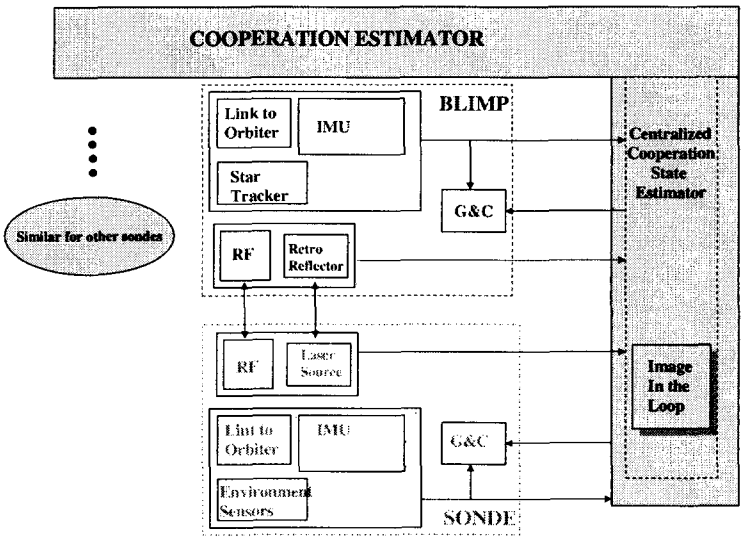

Figure 9. Elements of Cooperation Estimator.

In our current design, we simulate three sondes moving on the surface of Titan along with the blimp. The robots operate in a formation shown in figure 8. In order for the blimp to track and command the sondes to move in formation, it must continuously measure and estimate the location of each sonde. We adapted a distributed relative sensing scheme using cooperation sensor Ka-Band transceiver/patch antennas similar to that of the Global Positioning System (GPS). The antennas provide full duplex links of the range and bearing between any two units (blimp-to-sonde or sonde-to-sonde). This technology was developed for the autonomous formation flying (AFF) sensor platform and is shown to be able to measure relative ranges with a maximum uncertainty of 2 cm and measure bearing angles with a maximum uncertainty of 1 arcmin [2]. In the simulation, the RF metrology sensor measurement accuracy (1-σ) is of 4 mm in range and 0.3 milliradians in bearing. The assumed standard deviation of initial relative position knowledge error is 1.0 m. This implies an evolution of the current performance of the AFF sensor. The sensor measurements are then fed through a Kalman filter to generate estimates of the formation parameters. We show in simulation that a simple Kalman filter can effectively reduce the noise from the range and bearing measurements. Once the relative positions of the sondes are known, the blimp commands the sondes to move in formation and avoid obstacles using the potential field method.

The current implementation of the formation estimator estimates only the relative position of the herd elements. This implies that the measurements used depend only on relative position and are not correlated to other system state variables such as the attitude estimates of the elements or the misalignments (un-calibrated) between various subsystems. This assumption is acceptable only as long as the effects of these secondary disturbances are small compared to the errors in the relative position measurements (e.g. attitude estimate error is much less than metrology 'bearing' measurement uncertainty).

Herd Control – Potential Field

There has been a large body of work on motion planning and cooperative control of many robots. Our goal is to plan and control a number of sondes and blimp's motion from the initial positions to a moving or stationary target in a desired manner while avoiding possibly moving obstacles. To achieve this goal, we selected the potential field method for its simplicity and its low computational requirements. There are a number of variations on the potential field method [5][6][7]. One of the variations, virtual force field (VFF) [6], works best for real-time applications, and it is suited for the limited computational resources available on the sondes.

The VFF method uses attractive and repulsive potentials to generate actuator forces that smoothly drive the vehicle to a specified target while avoiding obstacles. The sondes and other obstacles can be represented as point particles on a Euclidean space at a fixed time. For each point particle *j* surrounding any given sonde *i*, a virtual force is asserted from particle *j* to sonde *i*. This virtual force has the form

$$F_{i,j}(X_i, X_j) = \left(\frac{c_{i,j}}{(r_{ij})^n} \right) \left(\frac{X_j - X_i}{r_{ij}} \right) \tag{19}$$

where X is the position of the particle. $r_{ij} = \|X_i - X_j\|$ is the Euclidean distance between point particle i and j, and $c_{i,j}$ is the coefficient for the force vector. $c_{i,j}$ can be positive if the force is attractive and negative if the force is repulsive. To ensure that the sondes do not collide with each other and other obstacles, each sonde is asserted with repulsive forces (negative $c_{i,j}$) from stationary obstacles and other moving obstacles, including neighboring sondes. Targets apply attractive forces (positive $c_{i,j}$) to guide the sondes toward the targets. The sondes can also assert attractive forces to each other when they are too far part and assert repulsive forces when they are too close to each other. This has the effect of keeping the sondes moving in a relatively tight formation while avoiding colliding to each other. The overall virtual force applied by the entire system on a sonde i is, therefore,

$$F_i = \sum_{j \neq i} F_{i,j}(X_i, X_j) \tag{20}$$

Results and Discussion

We simulated a complete system of the blimp and three sondes moving from target to target on the Titan Surface. The simulation is done using Matlab Simulink. The top level view of the simulation is shown in the following diagram. The Simulink model consists of control, dynamics, and sensor/estimator models for the blimp and the sondes.

The cooperation estimators and the potential field commands guide the sondes and the blimp to move in a synchronized fashion. Figure 10 shows the block diagram of the entire simulation. Each vehicle is simulated by an independent processor, for a total of four processors. The blimp dynamics, the cooperation estimator, and the potential field commander/controller, are located on a single blimp processor. The other processors are assigned to each sonde individually.

Figure 11 shows the results of a simulation representing the blimp turning 20 degrees in yaw to keep pointed to Earth while being buffeted by 1 m/s wind at 1 km altitude in the Titan's atmosphere. The peak lateral force that the propellers must counteract is ~3.6N along +Y, while the peak torque is ~60Nm along +Z. The total power required to execute the maneuver is about 10 Watts.

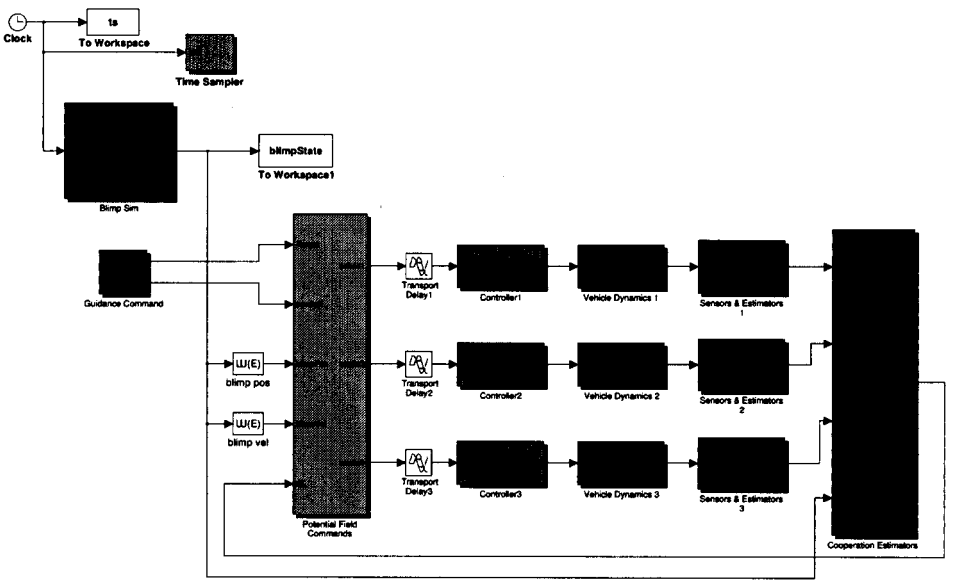

Figure 10. Matlab Simulink block diagram

We also created a scenario to command the sondes to move toward a common target and stay there for some time. At simulation time 80s, the blimp commanded the sondes to move toward the second target. At simulation time 160s, the sondes reached the second target. We placed obstacles at (1,1), (3,1), (5,2.5), and (7,1) on the x, y coordinate plane. The first target was located at (2,4), and the second target was located at (9,0). The initial starting positions of the sondes were (0,0), (3,0) and (0,3). See figure 12. Each sonde was able to maintain a minimum relative distance of 0.5(m) from adjacent sondes. See figure 13 for relative distances. The power consumption profile of the sondes is shown in figure 14. We also visualized the performance of the Kalman estimator by comparing the true relative range values from the dynamics with the estimated values. The result is shown in figure 15.

transport delay is inserted in between the potential field command block and the sonde controller. We observed degrading performance of the controller as we increased the input delay time. However, under a few seconds of delay, the sondes still managed to move around the obstacles and toward the target reasonably well. See figure 16 and 17.

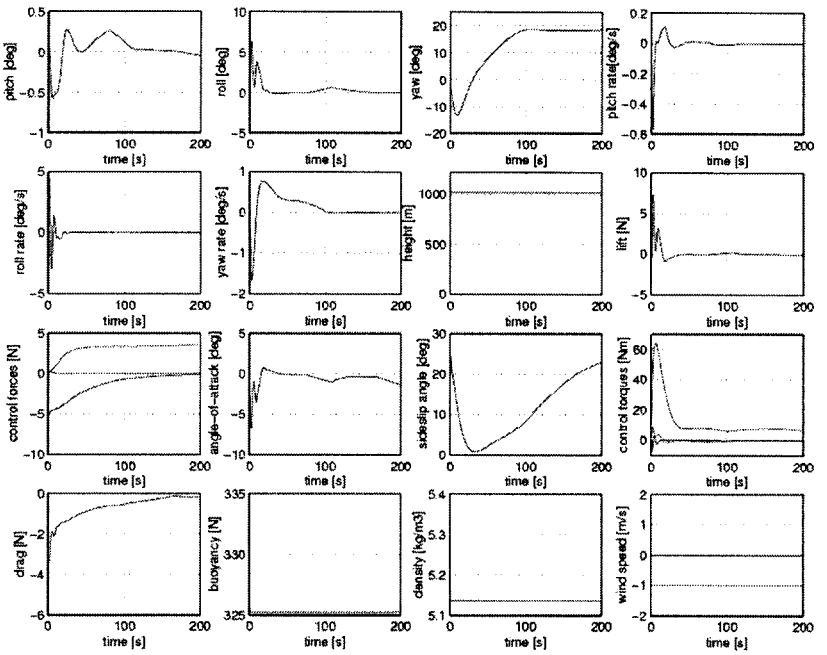

Figure 11. Turn of 20 degrees in yaw to keep blimp pointed to Earth while being buffeted by 1 m/s wind,

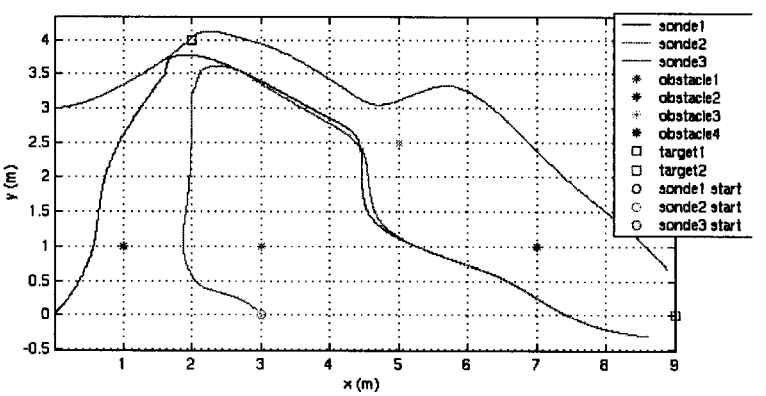

Figure 12. The paths of the sondes moving from target to target while avoiding obstacles.

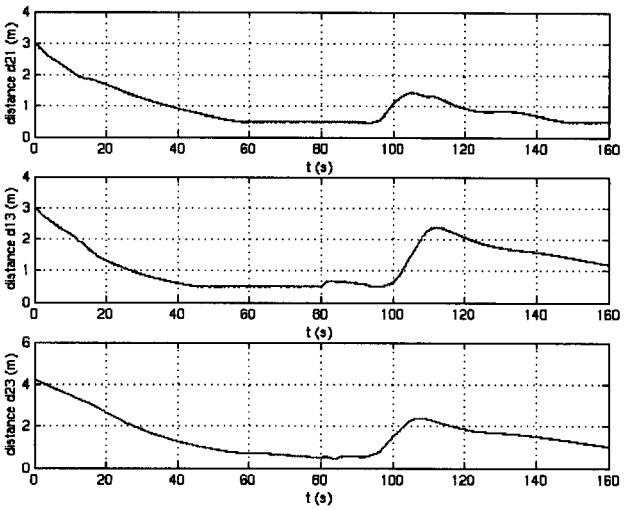

Figure 13. The relative sonde-to-sonde distances. The minimum sonde-to-sonde distance is set to 0.5(m).

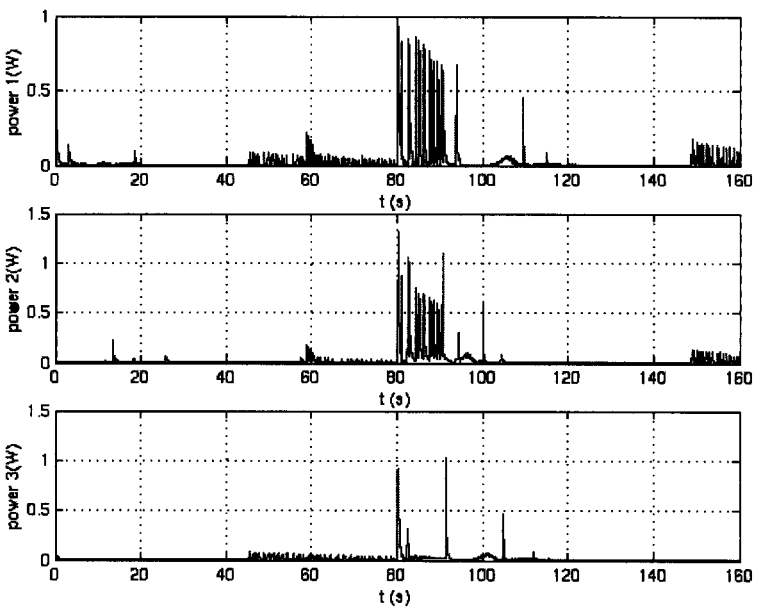

Figure 14. The power consumption profile of the sondes.

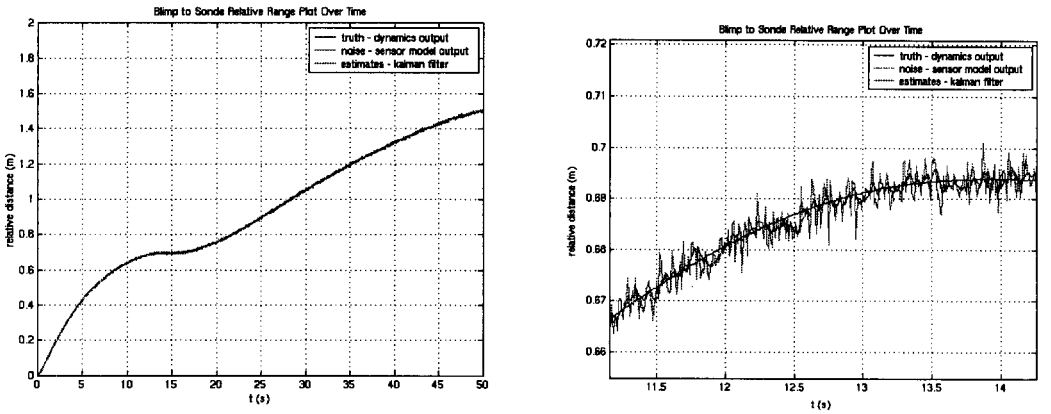

Figure 15. Relative range of one of the sondes to the blimp. The blue line is the ground truth generated from the dynamics. The green line is the noisy sensor model output; noise is added to the output from the dynamics according to our sensor model. The red line is the output from the estimator using the Kalman filter. The figure in the right is a blown-up version of the left one.

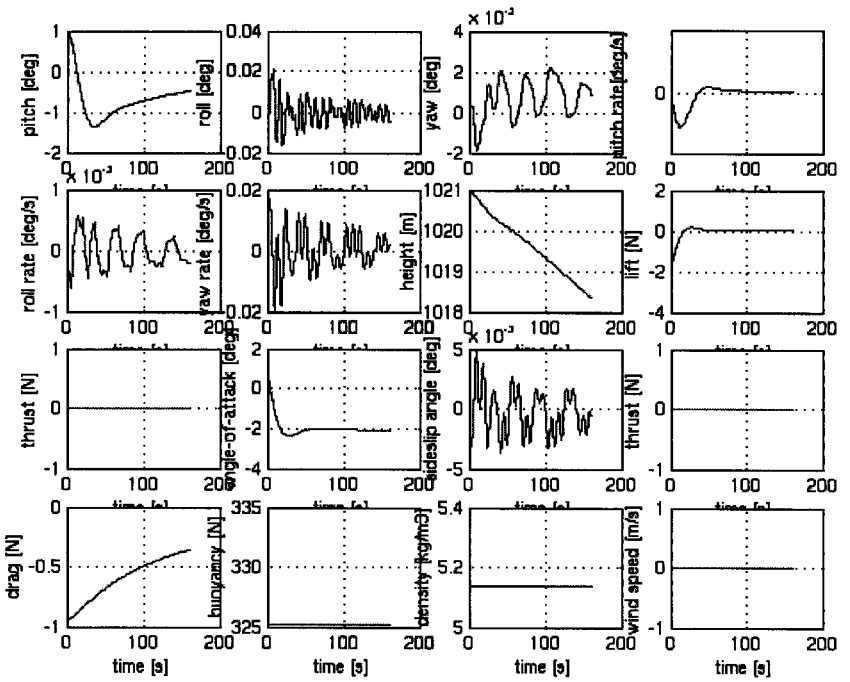

Figure 16. Blimp parameters output with input delay added in between the potential field command block and the sonde controller block.

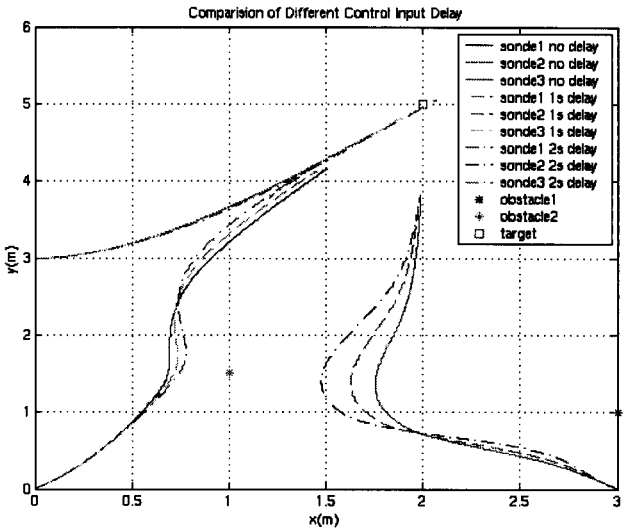

Figure 17. Paths of the sondes moving toward a target while avoiding obstacles under different input delays.

Conclusions

This paper has described the simulation model used to carry out design studies in herd guidance and control. First, the blimp model has been described. Second the sonde model has been described. Third, the integrated simulation environment has been described, with emphasis on the distributed sensing and actuation architecture used to command and control the herd of sondes. Finally, several simulation results have been analyzed. The result of simulation studies have demonstrated that the method used for commanding the herd (based on a potential field architecture), and for the distributed sensing of the herd based on transmitting and receiving radio-frequency signals amongst the vehicles is feasible even if significant uncertainty exists in the dynamics and environmental models. These results are very encouraging, and open the way to efficient autonomous control of many data gathering vehicles in totally unknown planetary environments.

Acknowledgments

This research was performed at the Jet Propulsion Laboratory, California Institute of Technology, under contract with the National Aeronautics and Space Administration. The authors are grateful to Mr. Pat Trauttman, manager of the RASC program at NASA HQ, Mrs. Marianne Rudisill, RASC manager at LaRC, Drs. Charles Weisbin, Jeff Hall, and Fred Hadaegh at JPL for financial and intellectual support in this task. The authors are also grateful to the other members of the RASC'03 team at JPL, (R. Manvi, W. Zimmermann, S. Chau, A. Sangupta) for providing a stimulating research environment.

References

[1] W. Zimmerman, S. Chau, M. Quadrelli, RASC Interim Report, July 2003.
[2] N. Sarkar, X. Yun, and V. Kumar, "Control of mechanical systems with rolling constraints: Application to dynamic control of mobile robots," Int. J. Robot. Res., vol. 13, no. 1, pp.55-69, 1994
[3] T. Fukao, H. Nakagawa, and N. Adachi, "Adaptive Tracking Control of a Nonholonomic Mobile Robot," IEEE Transactions on Robotics and Automation, Vol. 16, No.5, October 2000
[4] M. Aung, G. H. Purcell, J. Y. Tien, L. E. Young, L. R. Amaro, J. Srinivasan, M. A. Ciminera, and Y. J. Chong, "Autonomous Formation-Flying Sensor for the StartLight Mission," IPN Progress Report 42-152, Jet Propulsion Laboratory, Pasadena, California, February, 2003.
http://ipnpr.jpl.nasa.gov/tmo/progress_report/42-152/152A.pdf
[5] J. H. Reif, H. Wang, "Social Potential Fields: A Distributed Behavioral Control for Autonomous Robots," Robotics and Autonomous Systems 27 (1999) 171-194
[6] Y. Koren, J. Borenstein, "Potential Field Methods and Their Inherent Limitations for Mobile Robot Navigation," Proceedings of the 1991 IEEE International Conference on Robotics and Automation, Sacramento, California – April 1991
[7] P. Veelaert and W. Bogaerts, "Ultrasonic Potential Field Sensor for Obstacle Avoidance,", IEEE Transaction on Robotics and Automation, Vol. 15, No. 4, August 1999
[8] G. Welch and G. Bishop, "An Introduction to the Kalman Filter," http://www.cs.unc.edu/~welch/kalman/